

# 577 nm yellow laser source using external pumping

**Great Chayran**

Institute of Physics of the Czech Academy of Sciences

**Venkatesan Jambunathan** (✉ [jambunathan@fzu.cz](mailto:jambunathan@fzu.cz))

Institute of Physics of the Czech Academy of Sciences

**Martin Smrz**

Institute of Physics of the Czech Academy of Sciences

**Tomas Mocek**

Institute of Physics of the Czech Academy of Sciences

---

## Research Article

**Keywords:**

**Posted Date:** December 1st, 2022

**DOI:** <https://doi.org/10.21203/rs.3.rs-2320565/v1>

**License:**  This work is licensed under a Creative Commons Attribution 4.0 International License.

[Read Full License](#)

---

# Abstract

We demonstrated a 577 nm yellow laser source with a proper combination of Raman medium and frequency doubling medium, pumped externally. Cryogenic Yb:YAG oscillator acts as an external pump source and it generates 1.2 mJ energy at 1KHz emitting around 1029 nm. Using Raman resonator with  $\text{Ba}(\text{NO}_3)_2$  as Raman medium, SRS around 1153.4 was generated. Finally, 577 nm yellow laser was generated using the frequency doubling medium LBO. A maximum average output power of 65 mW with a pulse duration of 18 ns at 1 KHz was achieved.

## 1 Introduction

In recent years, diode pumped solid-state lasers have become ubiquitous due to their vast scientific and technological applications. Especially in the field of medicine, it finds numerous applications in general surgery, urology, dermatology, dentistry, ophthalmology etc. This was possible mainly because of the replacement of flash lamps with more efficient and cheaper laser-diode as pump sources, as well as the availability of solid-state laser gain media for a specific wavelength region. In addition, the more accurate spectral wavelength matching between diode laser emission and gain material's absorption leads to a significant benefit in laser efficiency and subsequently in compactness, reliability, and cost.

To date, lasers for applications in general surgery, urology, dentistry, dermatology etc., have been readily available. This is due to the availability of laser gain materials that can be emitted at particular wavelength for these applications [1]. Concerning the application in ophthalmology, especially for retinal photocoagulation treatment, a light source emitting at yellow wavelength region emitting at 577 nm is of great interest. This is because of the excellent absorption characteristics at this wavelength region [2]. Moreover, the peak absorption of oxyhemoglobin and negligible macular xanthophyll absorption at this wavelength region enable the ophthalmologist to perform retinal photocoagulation treatment with minimum risk and lower energy. However, achieving this 577 nm wavelength is not an easy task because of non-availability of proper gain media that emit at this particular wavelength. There are many other systems developed in the past emitting around 577 nm wavelengths such as semiconductor lasers or a dye lasers [3–8]. However, these lasers possess extreme technical complexities such as the dyes tend to degrade chemically during laser operation and semiconductor laser suffers from poor beam quality and high divergence of beam. In addition, these lasers either operates at continuous wave or long duration pulses (ms or  $\mu\text{s}$  pulses) resulting in thermal effect in the eye with associated collateral damage. Currently, 532 nm solid-state lasers are in use for these applications, even though they are not optimum for these applications [9]. To overcome these issues few ophthalmist proposed short pulses in the nanosecond regime emitting at 577 nm would be optimal [9, 10].

Taking into account all the above-mentioned facts, a yellow light source emitting at 577 nm with shorter pulses (ns) is a prerequisite. We explored several possibilities and demonstrated a yellow laser source emitting around 577 nm with a proper combination of gain, Raman, and frequency doubling media using intracavity pumping in one of our previous works [11]. As an alternative approach and for power

scalability, here in this work, we employed external pumping to generate the 577 nm wavelength, which is explained in the latter part of the session.

## 2 Experimental

### 2.1 Laser setup

The laser experiment was carried out using the setup mentioned in Fig. 1. It consists of an external pump source, a Raman resonator, and other optical elements to image the output of the pump source onto the Raman resonator. The external pump source is an in-house cryogenic Yb:YAG electro-optically Q-switched oscillator as demonstrated earlier in one of our previous works [12, 13]. The cryogenic Yb:YAG oscillator was constructed using several optical elements and the laser oscillated between two end mirrors. One end mirror being curved mirror with radius of curvature (ROC) 300 mm and other end mirror being flat mirror, both are high reflection (HR) coated for 1030 nm. To pass the pump light onto the gain media a dichroic mirror that was antireflection (AR) coated for 900–980 nm on the rear side and HR coated for 1020–1200 nm on the front side was used. As gain medium, an AR coated 3at.%Yb:YAG, 3mm thick and 10 mm aperture was mounted at normal incidence in a copper holder. To match the laser mode in the cavity a mode-matching lens with 150 mm focal length AR coated for 1030 nm was used. A thin film polarizer with a quarter-wave plate acts as a variable output coupler. As electro-optic Q-switching element, a BBO pockels cell was used. To pump the crystal a fiber-coupled laser diode, which has a capacity of delivering 25 W, was used. The fiber has a core diameter of 200  $\mu\text{m}$  and 0.22 NA and was Volume Bragg grating (VBG) stabilized with 0.35 nm linewidth and emits around 968.7 nm. To image the pump light from the fiber output to the gain media, two AR coated achromatic lenses of focal lengths 150 mm and 200 mm were used. The gain media Yb:YAG was conduction cooled using the liquid helium cryostat (Cryodyne, model no: 22C) and the temperature of the sample was maintained at 120 K which was found to be optimal for efficient cryogenic laser operation under given experimental condition [13].

To transport the Q-switched laser output from our external pump source to the Raman resonator several optical elements were used. Firstly, a telescope was built to make a collimated pump beam using two plano-convex lenses each having a focal length of 125 mm. Secondly, to focus the collimated beam to the Raman resonator a 200 mm plano-convex lens was used. Finally, in order to prevent the back-reflected light from the Raman resonator an optical isolator after the pump source was placed. The pump mode size on the Raman resonator was estimated to be around 260  $\mu\text{m}$  in diameter.

The Raman resonator employs a hemispherical cavity consisting of a flat pump mirror and a concave output coupler. The flat mirror was HR coated around 1130 to 1200 nm and High transmission coated around 1010 to 1060 nm. The output coupler mirrors has ROC of 100 mm and have different transmissions of output coupling with ( $T_{oc} = 1, 3, 5$  and 10% @ 1100–1180 nm and 75% @ 577 nm). For Raman generation a  $\text{Ba}(\text{NO}_3)_2$  crystal AR coated around 1064–1198 nm was placed in between the two mirrors. Two  $\text{Ba}(\text{NO}_3)_2$  crystals that have the dimensions of 20 mm and 50 mm in length with 5\*5mm<sup>2</sup> aperture respectively were studied for the Raman generation. It has the Raman shift of 1048  $\text{cm}^{-1}$  that

enables the generation of 1154 nm intermediate wavelength [14]. To generate the 577 nm, a frequency doubling medium Lithium Triborate ( $\text{LiB}_3\text{O}_5$ ) which was 10 mm in length and  $3 \times 3 \text{ mm}^2$  aperture, AR coated and phase matched for  $\Theta = 90^\circ$ ,  $\Phi = 5.4^\circ$  at room temperature were used. The advantages of LBO crystals are that it exhibits very broad transparency, small walk-off angle, high damage threshold, and noncritical phase matching capability [15].

For detecting the pulses, silicon photodiode model no (ET-2020) was used. The signal was recorded using the 600 MHz oscilloscope (Teledyne Lecroy wave surfer 64Mxs-B). For detecting the fundamental, Raman and yellow wavelength compact spectrometers (model no Wavescan USB for Raman spectrum, Thorlabs CCS200 for visible region and Ocean Optics USB2000 + for Pump laser spectrum) were used. For measuring the beam, profile a universal beam profiler (KLT-UBP) was used. Thorlabs S401C thermal power sensor was used to measure the yellow and Raman laser power and Ophir pyroelectric Laser sensor PE25-C energy meters was used to measure the pump laser pulse energy. A long pass filter (Thorlabs- FEL 1100) to filter the Raman laser output and a band pass filter (Altechna - Filtr SZS-21) to filter the yellow laser output were used.

## 3 Results And Discussion

### 3.1 Cryogenic Yb:YAG oscillator

Initially, the continuous-wave laser oscillation was realized. After optimizing the distance between two end mirrors, BBO crystal was inserted. With proper alignment of BBO pockel cell with required half-wave voltage and adjusting the position of the quarter wave plate, Q-switched pulses were generated at 1KHz repetition rate. Figure 2a) shows the incident power vs average output power characteristics of the cryogenic Yb:YAG oscillator. The pulse energy increases with increase of incident power and a maximum pulse energy of 1.2 mJ was achieved. Further power scaling was not carried out in order to prevent the damage of optical elements.

Figure 2b) shows the evolution of pulse width for different pulse energy of the cryogenic Yb:YAG oscillator. From the figure, one can observe a longest pulse width of 70 ns for 0.5 mJ energy and shortest pulse width 32 ns for 1.2 mJ energy. We also measured a very good Gaussian beam profile of the pump beam in the far field, which is shown in Fig. 2c). The cryogenic laser Yb:YAG oscillator emits around 1029 nm at 120K.

### 3.2 Raman laser

Stimulated Raman scattering (SRS) was realized by pumping the  $\text{Ba}(\text{NO}_3)_2$  Raman medium using the hemispherical cavity as mentioned in the experimental session. Two different lengths 20 mm and 50 mm were studied. The cavity length with 20 mm long Raman medium was around 40 mm and with 50 mm Raman medium, the cavity length was around 65 mm. Using ABCD matrix formalism [16], the mode size with 40 mm long cavity was estimated to be around 260  $\mu\text{m}$  and with 65 mm long cavity the mode size was estimated to around 270  $\mu\text{m}$ .

Figure 3a) and 3b) shows the input vs SRS output power characteristics with 20 mm and 50 mm long Raman medium respectively for various Tocs. From the figures, one can infer that output power increases non-linearly with an increase in input power [12]. In both the cases, Toc 5% performed better and generates highest output power. With 20 mm Raman crystal, a maximum output power of 256 mW with optical-to-optical efficiency of 21.3% was achieved. A slightly higher output of 319 mW with optical-optical-efficiency of 26.5% for 50 mm Raman crystal was achieved. Although the Raman length is more than doubled from 20 mm to 50 mm, we could improve the output power by less than 25%. This is because of the mismatch between the pump and laser mode as the cavity length increases. The SRS emits at 1153.4 nm for all the output couplers used. The SRS pulse width amounts to 18 ns for both the crystals irrespective of the increase of incident pump power.

### 3.3 577 nm yellow laser

The yellow (577 nm) laser was generated by placing 10 mm long frequency doubling crystal LBO after the Raman crystal inside the cavity. For the experiments, the same Toc's were utilized as in the Raman experiments. We tried to achieve the yellow laser with both the Raman crystals and with all the output couplers. We succeed in achieving the required yellow laser wavelength around 577 nm and the obtained laser results were summarized in Fig. 4a and 4b.

Figure 4a) shows the input power vs yellow output power characteristics of the resonator configuration consisting of 20 mm Raman crystal along with 10 mm LBO. After inserting the LBO, the cavity length increased to 40 mm. The laser mode size on this configuration was estimated to be around 258  $\mu\text{m}$ . From the figures, one can infer that out of all the couplers used, the Toc1% performed better. A maximum output power of 65mW with optical-to-optical efficiency of 5.4% was achieved. Figure 4b) shows the input power vs yellow output power characteristics of the resonator configuration consisting of 50 mm Raman crystal along with 10 mm LBO. The cavity length in this configuration was 65mm and resonator mode size was 270  $\mu\text{m}$  microns. Here again Toc 1% performs better when compared to other Tocs. A maximum output power obtained was 21 mW with an efficiency of 1.75%. The better performance with Toc 1% is attributed to high intracavity power inside the Raman resonator, which in turn improves the second harmonic efficiency inside the cavity. Also better output power with 20 mm configuration is the result of better mode matching. The yellow laser emits around 576.7 nm and the pulse width amounts to 18 ns. Figure 4c) shows the far-field Gaussian profile of yellow laser. Figure 4d) shows the measured pump, Raman and yellow laser wavelength during the experiment.

## 4 Conclusions

As a proof of principle, we demonstrated a 577 nm yellow laser source with a proper combination of Raman medium and frequency doubling medium, pumped externally. The pump source was an in-house cryogenic Yb:YAG oscillator generating 1.2 mJ energy at 1 KHz. Using the Raman resonator, the Raman medium,  $\text{Ba}(\text{WO}_4)_2$  with two different lengths 20 mm and 50 mm were characterized. In the end, a yellow laser around 576.7 nm was generated. A maximum output power of 65 mW with a pulse duration of 18

ns at 1 KHz corresponding to an optical-to-optical efficiency of 5.4% was achieved. This preliminary experimental result motivates us to explore further possibilities such as changing the cavity design to better utilize the longer Raman and LBO crystals and to use powerful nanosecond pump lasers emitting around 1030 nm, which we plan to do next.

## Declarations

### Acknowledgments

This work was co-financed by the European Regional Development Fund and the state budget of the Czech Republic (project HiLASE CoE: Grant No. CZ.02.1.01/0.0/0.0/15\_006/0000674) and by the European Union's Horizon 2020 research and innovation programme under grant agreement No. 739573.

## References

1. K. Scholle, S. Lamrini, P. Koopmann, and P. Fuhrberg, in *Frontiers in Guided Wave Optics and Optoelectronics*, Ch. 21, ed. by B. Pal (INTECH Open Access Publisher, Rijeka, 2010)
2. G. Staurengi, *RETINA TODAY* **31** (2016).
3. R. Bornemann, U. Lemmer, and E. Thiel, *Opt. Lett.* **31**, 1669 (2006).
4. O. G. Peterson, S. A. Tuccio, and B. B. Snavely, *Appl. Phys. Lett.*, **17**, 245 (1970).
5. R. Bornemann, E. Thiel, and P. H. Bolívar, in *Organic Photonics V*, edited by B. P. Rand, C. Adachi, and V. van Elsbergen (SPIE, 2012), p. 84351F.
6. A. Sahm, N. Werner, J. Hofmann, R. Bege, and K. Paschke, *IEEE Photonics Technol. Lett.* **30**, 1878 (2018).
7. J. Lin, H. M. Pask, D. J. Spence, C. J. Hamilton, and G. P. A. Malcolm, *Opt. Express* **20**, 5219 (2012).
8. E. Kantola, A. Rantamäki, I. Leino, J.-P. Penttinen, T. Karppinen, S. R. Mordon, and M. Guina, *IEEE J. Sel. Top. Quantum Electron* **25**, 1 (2019).
9. J. P. M. Wood, M. Plunkett, V. Previn, G. Chidlow, and R. J. Casson, *Lasers Surg Med* **43**, 499 (2011).
10. K. Aflalo, M. Ben-David, A. Stern, and I. Juwiler, *OSA Contin* **3**, 3253 (2020).
11. V. Jambunathan, S. P. David, F. Yue, X. Mateos, O. Novak, M. Smrz, and T. Mocek, in *2021 Conference on Lasers and Electro-Optics Europe and European Quantum Electronics Conference*, OSA Technical Digest (Optica Publishing Group, 2021), paper ca\_p\_10.
12. V. Jambunathan, T. Miura, L. Těsnohlídková, A. Lucianetti, and T. Mocek, *Laser Phys. Lett.* **12**, 15002 (2014).
13. V. Jambunathan, L. Horackova, P. Navratil, A. Lucianetti, and T. Mocek, *IEEE Photonics Technol. Lett.* **28**, 1328 (2016).
14. H. M. Pask, *Prog. Quantum electronics* **27**, 3 (2003).

15. Y. M. Andreev, M. Naftaly, J. F. Molloy, A. E. Kokh, G. v Lanskii, V. A. Svetlichnyi, V. F. Losev, N. G. Kononova, and K. A. Kokh, *Laser Phys. Lett.* **12**, 115402 (2015).
16. N. I. Chunosov, "Rezonator2," 2020, <http://rezonator.orion-project.org/>.

## Figures

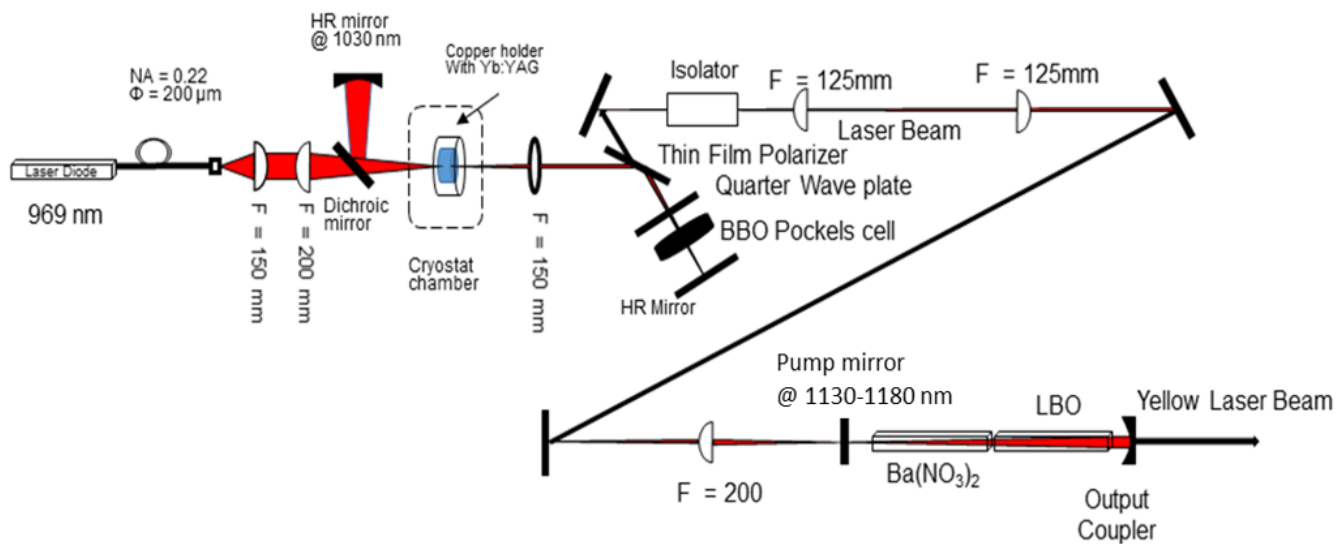


Figure 1

Schematic of the laser setup for the generation of 577 nm.

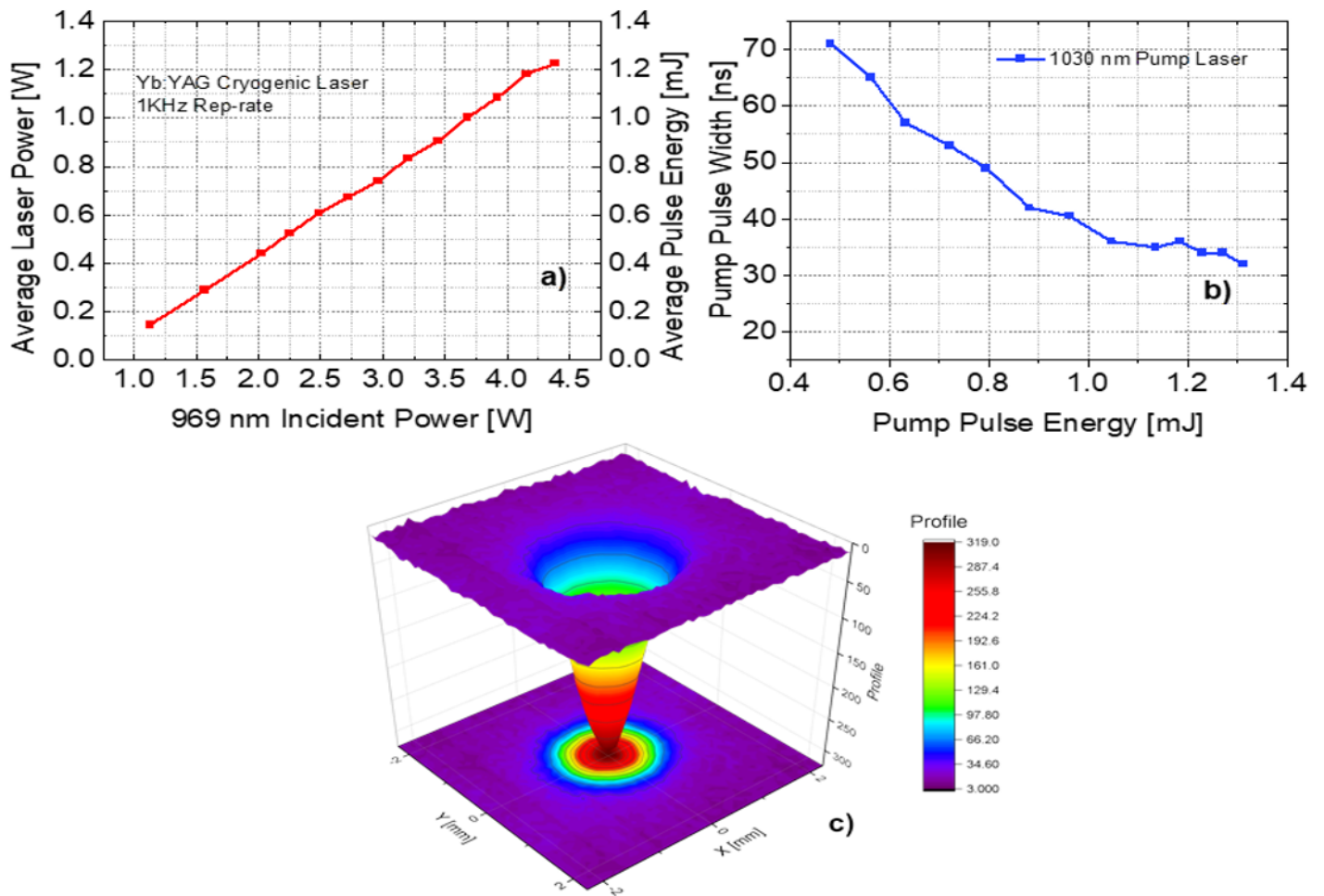


Figure 2

a) Incident power vs average output power at 1KHz rep-rate. b) Evolution of pulse width with different pulse energy. c) Far-field Gaussian beam profile of cryogenic Yb:YAG oscillator.

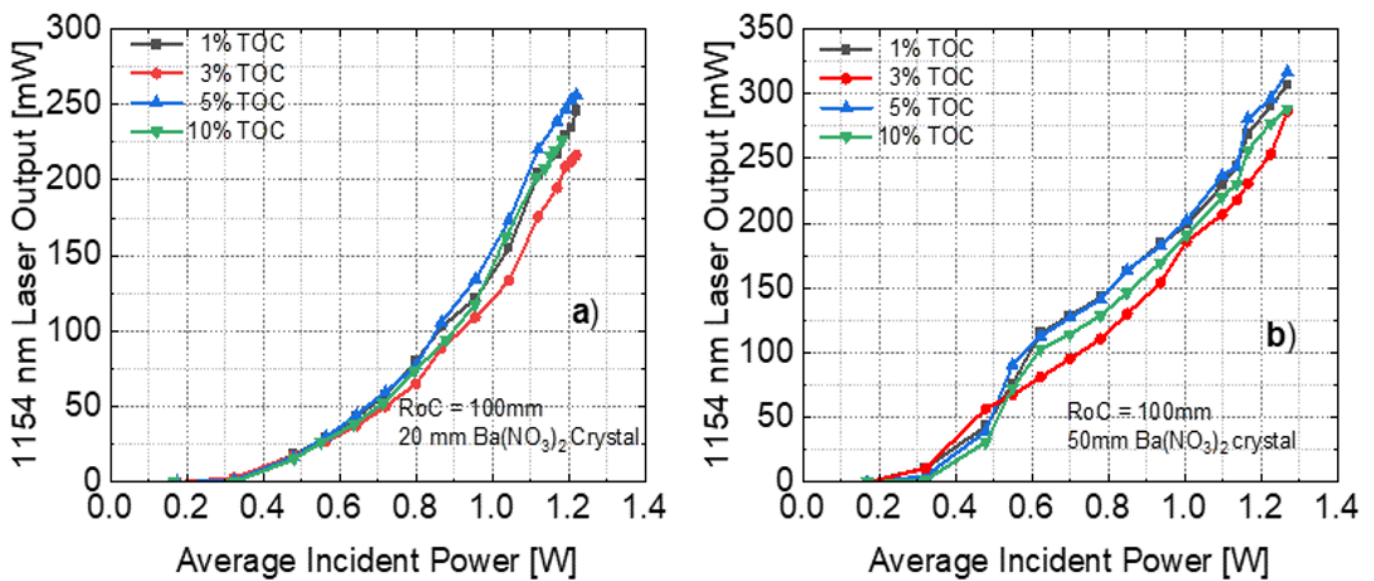




Figure 3

a) Input power vs SRS output power characteristics with 20 mm Raman medium. b) Input power vs SRS output power characteristics with 50 mm Raman medium.

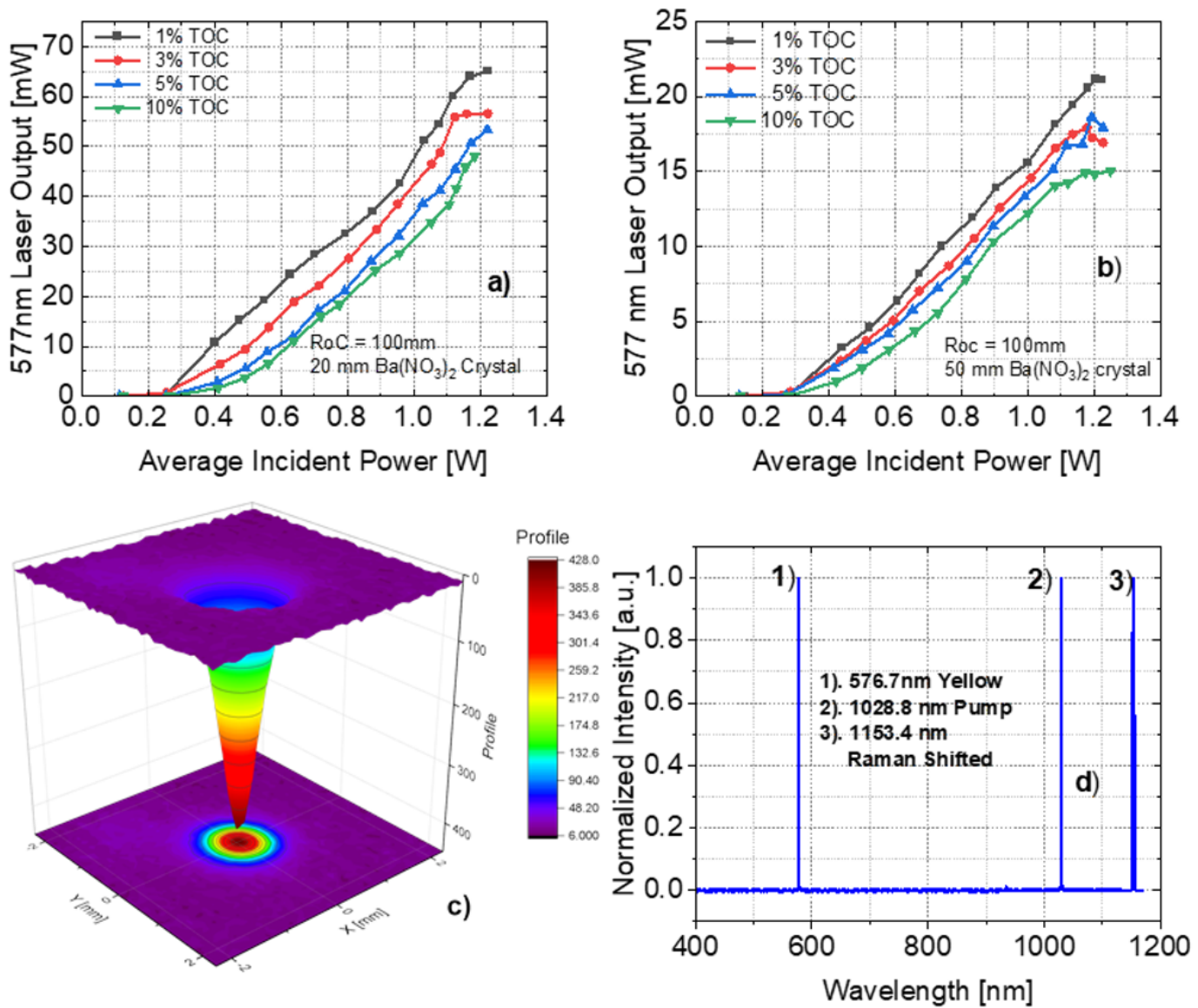


Figure 4

a) Input power vs yellow output power characteristics for 20 mm Raman medium and 10 mm LBO. b) Input power vs yellow output power characteristics for 50 mm Raman medium. c) Far-field Gaussian beam profile yellow laser. d) Measured Pump, Raman, and yellow laser wavelengths.